Journal of Steroid Biochemistry & Molecular Biology 117 (2009) 107–116

Contents lists available at ScienceDirect

Journal of Steroid Biochemistry and Molecular Biology

journal homepage: www.elsevier.com/locate/jsbmb

Overexpression of *Nrp/b* (nuclear restrict protein in brain) suppresses the malignant phenotype in the C6/ST1 glioma cell line

Theri Leica Degaki, Marcos Angelo Almeida Demasi, Mari Cleide Sogayar*

Departamento de Bioquímica, Instituto de Química, Av. Prof. Lineu Prestes 748, Sala 964, Universidade de São Paulo, 05508-900 São Paulo, Brazil

ARTICLE INFO

Article history:
Received 3 September 2008
Received in revised form 28 July 2009
Accepted 29 July 2009

Keywords:
Nrp/b (nuclear restrict protein in brain)
Nrp/b overexpression
C6/ST1 cell line
Suppression of the tumoral phenotype

ABSTRACT

Upon searching for glucocorticoid-regulated cDNA sequences associated with the transformed to normal phenotypic reversion of C6/ST1 rat glioma cells, we identified *Nrp/b* (nuclear restrict protein in brain) as a novel rat gene. Here we report on the identification and functional characterization of the complete sequence encoding the rat NRP/B protein. The cloned cDNA presented a 1767 nucleotides open-reading frame encoding a 589 aminoacids residues sequence containing a BTB/POZ (broad complex Tramtrack bric-a-brac/Pox virus and zinc finger) domain in its N-terminal region and kelch motifs in its C-terminal region. Sequence analysis indicates that the rat *Nrp/b* displays a high level of identity with the equivalent gene orthologs from other organisms. Among rat tissues, *Nrp/b* expression is more pronounced in brain tissue. We show that overexpression of the *Nrp/b* cDNA in C6/ST1 cells suppresses anchorage independence *in vitro* and tumorigenicity *in vivo*, altering their malignant nature towards a more benign phenotype. Therefore, *Nrp/b* may be postulated as a novel tumor suppressor gene, with possible relevance for glioblastoma therapy.

1. Introduction

Gliomas have been pathologically defined as tumors which display histopathological, immunohistochemical and ultrastructural evidence of glial differentiation [1]. Four malignancy grades are recognized by the WHO (World Health Organization), with grade I tumor being the biologically least aggressive and grade IV, the most aggressive tumors [2–4]. The carcinogenesis of gliomas, particularly the molecular defects which underlie initiation and progression of these tumors, is ill-defined [5], hampering the development of successful therapies for gliomas [6]. Gene therapy is a viable option for the treatment of malignant brain tumors, although no ideal vector has yet been developed [7]. Model organisms are important in the study of gliomas as well in testing targeted therapeutics. The widely employed rat brain tumor models [8], have provided a wealth of information on the biology, biochemistry and experimental therapeutics of brain tumors in experimental neuro-oncology [9,10].

The rat C6 glioma cell line is an experimental model system for glioblastoma (GBM) growth, invasion and metastasis and for the design and evaluation of anticancer therapies [11]. Growth of the C6 rat glioma cell line is inhibited by glucocorticoid hormones (GC) [12,13]. These hormones constitute a class of corticosteroids produced by the adrenal gland, being routinely prescribed for patients with brain tumors [14] to decrease edema [15] and, also, due to their anti-neoplastic capabilities [16]. GC enters the cells through passive diffusion and forms a complex with the glucocorticoid receptor (GR) protein. The GC–GR complex then undergoes activation and enters the cell nucleus, where it binds to the DNA, leading to a number of biological responses induced by these hormones [17].

To study the molecular mechanisms of GC as an anti-tumor agent in glioma cells, we have previously isolated the C6/ST1 variant [18] from the C6 rat cell line [19]. This variant is hyperresponsive to GC, going from a fully transformed and tumorigenic phenotype to a normal one, both *in vitro* and *in vivo* [18]. Using different techniques, we found several GC-regulated genes which are associated with the transformed to normal phenotypic reversion that occurs in the C6/ST1 variant [20–22], among which we identified the *Nrp/b* gene [21], with a single transcript of approximately 5.5 kb, which is induced upon a 5 h treatment with hydrocortisone.

Recently, a human and mouse nuclear matrix protein NRP/B (nuclear restricted protein/brain) [23,24], also termed ENC-1 [25] or PIG10 [26], a member of the BTB/Kelch repeat family, was shown to be expressed in the nucleus, as a component of the nuclear matrix, in neuronal cells. The nuclear matrix, discovered in 1974 by Berezney and Coffey [27], plays a pivotal role in processing of genetic information [28], acting on transcription, RNA splicing/transport, DNA replication and repair [29,30]. Transcription factors including tumor supressors (e.g., Rb, p53) and hormone receptors (estrogen receptor), dynamically associate with specific nuclear matrix sites that support their assembly into functional macromolecular complexes [31]. Nuclear changes,

* Corresponding author. Tel.: +55 11 3091 3820; fax: +55 11 3091 3820.
E-mail address: mcsoga@iq.usp.br (M.C. Sogayar).

0960-0760/$ – see front matter © 2009 Elsevier Ltd. All rights reserved.
doi:10.1016/j.jsbmb.2009.07.009

such as alterations in nuclear shape, chromatin rearrangements and altered expression patterns of nuclear matrix proteins have recently been mechanistically linked to functional changes that promote tumor development [32]. The nuclear matrix coordinates different processes occurring at chromatin sites, which are under stringent control during the cell cycle [33]. Expression of this *Nrp/b* gene is rendered constitutive by overexpression of TP53 in the DLD1 colorectal cancer cell line [26], its expression being induced in neuroblastoma cells upon treatment with retinoic acid [23] and in adipocytes in response to the phosphodiesterase inhibitor methylisobutylxanthine [34]. The BTB-domain, localized at the N-terminal region of NRP/B, has been proposed to mediate protein–protein interactions, with 5–10% of human zinc finger proteins being estimated to contain these domains [35]. Recently, the BTB-domain of NRP/B has been described as an important regulator of neuronal differentiation [36]. The six copies of Kelch repeats in the C-terminal region of NRP/B are important for cytoskeletal organization and function [37] and mutations in this region are found both in brain tumor cell lines and in primary GBM tissues [38]. More importantly, in this same study, NRP/B mutations in the kelch domain conferred cell growth advantage by elevating ERK activation, suppressing cellular apoptosis in response to stressful stimulus by inhibiting TP53-mediated caspase activation and reducing its binding affinity to actin. Abundant expression of *NRP/B* was observed in several brain cell lines and in human brain tumors, including glioblastomas and astrocytomas [24], but alterations and gene mutations were found in these samples. These alterations may contribute to brain tumorigenesis by promoting cell proliferation and suppressing cellular apoptosis [38]. More recently, novel roles for *Nrp/b*, related to the oxidative stress response in breast cancer cells via the Nrf2 pathway [39,40], ovulatory process in rat [41] and modulation of Nrf2-mediated NQO1 induction against ROS-induced and proinflammatory damages in brain tumors[42], have been discovered.

Here, we report on the cloning and functional characterization of the rat full-length cDNA corresponding to the *Nrp/b* gene associated with phenotypic reversion of glioma C6/ST1 cells.

2. Materials and methods

2.1. Database homology searching and computational sequence analysis

Similarity searching was carried out on the GenBank rat genome draft sequence database (http://www.ncbi.nlm.nih.gov/) using BLAST tool [43]. Gene prediction analysis based on the genomic sequences and determination of the splice and acceptor site sequences of the NRP/B genomic DNA was performed using the BLAT tool (http://genome.ucsc.edu) from the University of California at Santa Cruz [44]. Multiple alignments between rat Nrp/b protein and its ortholog sequences were performed using the CLUSTAL W multiple alignment program, version 1.8 [45].

2.2. Culture conditions, RNA extraction and Northern blot analysis

C6/ST1 cells [18,46] were grown in Dulbelcco's modified Eagle's medium (DMEM—high glucose) (Gibco, MD, USA), supplemented with 5% fetal bovine serum (FBS) (Cultilab, Campinas, Brazil), 25 μg/ml ampicillin, 100 μg/ml streptomycin and 1.2 g/l sodium bicarbonate, in a humidified atmosphere containing 2% CO_2 in air, at 37 °C.

RNA was extracted from exponentially growing rat C6/ST1 cells. Cells were plated onto 100 mm diameter Petri dishes and maintained in either 5% FCS–DME or in 0.2% FCS–DME for 24 h (serum-starved synchronized cultures), before treatment with glucocorticoid (Hy 100 ng/ml). Total RNA was prepared according to Ref. [47], and quantified by spectrophotometry. Samples (20 μg) of total RNA were fractionated by electrophoresis in a 1.2% agarose–formaldehyde gel and transferred to nylon membranes (Life Technologies, Gaithersburg, MD, USA). Filters were hybridized to ^{32}P-labeled cDNA fragments of *Nrp/b* and/or 36B4 (ribosomal protein) used to control for the amount of RNA loaded onto the gel. DNA fragments were purified using the GFX kit (GE Healthcare, UK) and labeled with [α-^{32}P] dCTP (DuPont NEN, Boston, MA, USA) with the Ready-To-Go DNA Labelling Beads (-dCTP) (GE Healthcare, UK). After hybridization the membranes were exposed to phosphor-storage screens for 24 h prior to detection in the STORM 840 Phosphor Imager. Quantification and average lane background subtraction was performed using the ImageQuant (GE Healthcare, UK) software.

2.3. Cloning of the rat Nrp/b cDNA

DNA sequences named ESTs (expressed sequence tags), corresponding to putative rat orthologs of *Nrp/b*, were identified with a significant homology in a BLAST search of the GenBank nucleotide sequence databases, using the human and mouse *NRP/B* sequences. For the amplification of the 5′-terminal cDNA fragment, we used a sense primer 5′GGGGCGGCCTAATAATTTATTGACCTT3′, while the antisense primer 5′GGGGCGGCCGCCTAATAATTTATTGACCTT3′ was used to determine the 3′-end cDNA region. To obtain the full-length sequence of the *Nrp/b*, long-distance RT-PCR was performed using a library of cDNAs isolated from C6/ST1 cells as the template and Platinum High Fidelity TaqDNA Polymerase (Invitrogen, CA, USA). Specific primers for the 5′ (5′GCAGTCGACCACCATGTCCGTCAGCGTGCATGAGAA3′) and 3′ (5′AAAAGCGGCCGCATTAGGAAGGCAGGTGTTT3′) ends of the rat *Nrp/b* coding region were used to amplify the *Nrp/b* cDNA using polymerase chain reaction (PCR) with cDNA template derived from C6/ST1 cells treated with Hy for 5 h. The total RNA pool of C6/ST1 cells treated with Hy for 5 h was reverse transcribed using Superscript II reverse transcriptase (Invitrogen, CA, USA). The amplified fragment corresponding to the coding sequence of *Nrp/b* was cloned into the pLPCX retroviral vector (Clontech, CA, USA), resulting in a plasmid carrying the coding region of the rat *Nrp/b* cDNA, named pLPCX-NRP/B.

2.4. DNA sequencing and analysis

Sonicated fragments cloned into the pENTER 2B vector (Invitrogen, CA, USA) corresponding to different regions of the full-length cDNA of rat *Nrp/b* were sequenced using the vector forward and reverse primers. The sequencing reaction was performed using the DYEnamicTM ET dye terminator cycle sequencing kit (GE Healthcare, UK) and sequenced using the a ABI 3700 (PerkinElmer). The working draft sequences from automatic sequencing were assembled into a complete contiguous sequence using the Phred Phrap Consed program [48–50].

2.5. Rat Nrp/b gene expression analysis

A rat MTC panel (Clontech, CA, USA) containing cDNAs from several tissues (heart, brain, spleen, lung, liver, skeletal muscle, kidney and testis) was used for this study. The expression levels of *Nrp/b* were determined by qRT-PCR analysis. Primers were designed to amplify 100–150 bp length amplicons, with a melting temperature of 60 °C. *Nrp/b* sense primer 5′CTGGCAATGGAAGAACTCATCAC3′ and antisense primer 5′GACCACGCCGTCATTCTGTA3′ and *Gapdh* sense primer 5′CATGGCCTTCCGTGTTCCTA3′ and antisense primer 5′CCTGCTTCACCACCTTCTTGA3′ were employed. Quantitative data

were normalized relative to the internal housekeeping control glyceraldehyde 3-phosphate dehydrogenase (*Gapdh*) gene. Reactions resulting from the SYBR Green I Master Mix (Applied Biosystems, CA, USA), in the presence of cDNAs and forward and reverse primers (final concentration of 600 nM) were run on an ABI 7300 sequence detector (Applied Biosystems, CA, USA). The cycling conditions comprised a 10 min period of polymerase activation at 95 °C, and 40 cycles at 95 °C for 15 s, and at 60 °C for 1 min. The $2^{-\Delta\Delta Ct}$ equation was applied to calculate the relative expression of *Nrp/b* in tissues samples versus heart tissue where ΔCt = Ct gene − Ct GAPDH, and $\Delta\Delta Ct = \Delta Ct$ tissues − ΔCt heart [51]. The qRT-PCR runs for each sample were performed in duplicate and repeated when the Ct values were not similar. The results are presented in log 10 scale for better visualization.

2.6. Retroviral vector production

The pLPCX-NRP/B construct, pLPCX-EGFP plasmid (generously provided by Dr. Marcos Demasi from our laboratory) and pLPCX empty vector were transfected into the ϕnx-Ampho packaging cells (ATCC product SD 3443—Dr. Gary P. Nolan, Stanford University, CA) using Lipofectamine 2000 Reagent (Invitrogen, CA, USA), according to the manufacturer's protocol.

2.7. Transduction of C6/ST1 cells

Retroviral targeting experiments on rat glioma cell line were performed using a multiplicity of infection (MOI) of 100 based on the retroviral titer on NIH3T3 cells. C6/ST1 cells were incubated twice for 6 h with viral stocks collected from producer cells grown for 24 h, in the presence of 8 μg/ml polybrene (Sigma, MO, USA) in culture medium. Resistant cells were selected with 3.0 μg/ml Puromycin (Invitrogen, CA, USA) for 3 days, generating the C6/ST1-NRP/B, C6/ST1-EGFP and C6/ST1-pLPCX cells.

2.8. Growth curves

Cells (5.0×10^4) were plated onto 35 mm plates in 5% FCS–DMEM. In the following day, the cultures were washed twice with PBS and the medium was changed to either 0.5 or 5% FCS–DMEM. Duplicate plates were collected by trypsinization at the indicated periods of times and the cells were fixed in 3.7% formaldehyde, and counted in a CELM CC-530 electronic cell counter (São Paulo, Brazil).

2.9. Soft-agar assay

Cells suspended in 0.3% agar/10% FCS–DMEM medium were plated at a low cell density (250 cells/cm^2), onto previously coated plates containing with 0.6% agar in 10% FCS–DMEM. Upon gellification, liquid medium was carefully placed over the soft-agar layer and was replaced, by aspiration, every 3 days. Colonies were observed after 2 weeks and counted under a phase-contrast Nikon Diaphot microscope.

2.10. In vivo tumorigenesis assay

Six- to eight-week-old athymic (nu/nu) BALB/c nude mice were randomly divided into 4 groups, 4 in each group ($n = 2$). All animals were maintained in a sterile environment. Cages, bedding, food and water were autoclaved, and animals were maintained on a daily 12-h light/12-h dark cycle. The experimental group (C6/ST1-NRP/B), the vectors control (C6/ST1-EGFP and C6/ST1-pLPCX) and the untransfected C6/ST1 cells were separately injected subcutaneously (2.0×10^6 cells/mouse) in 100 μl of serum-free DMEM medium. Tumor dimensions were determined weekly using a caliper, and tumor volume was calculated as (the shortest diameter)^2 × (the longest diameter) × 0.5, and expressed in cubic millimeters [52]. Tumor growth rates were calculated as the change in tumor volume from weeks 1–6 (mm^3/week).

2.11. Whole protein cell extracts

Cells were plated onto 100 mm plates in 5% FCS-DMEM. In the following day, plates were washed with cold PBSA and then scrapped in the same solution. The cell suspensions were pelleted for 5 min at 200 × g at 4 °C. Cells were ressuspended in RIPA$^+$ buffer (10 mM Tris–HCl pH 7.5, 1% sodium deoxycholate, 1% NP-40, 150 mM NaCl, 0.1% SDS, 1 mM DTT, 1 mM PMSF, 1 μg/ml aprotinin, 5 μg/ml leupeptin, 1 μg/ml pepstatin and 10 mM NaF) and incubated on ice for 15 min. Cellular debris were removed by centrifugation (20,000 × *g*) for 30 min at 4 °C and the extract was stored at −70 °C. Protein concentrations were determined using the Bradford assay.

2.12. Western blotting

Cell lysates containing 30 μg of protein were loaded and fractionated onto 12% SDS-polyacrylamide gels and were transferred to nitrocellulose membranes by electroblotting. Pounceau S staining of the blots was adopted to ensure equivalent loading. The nitrocellulose membranes were incubated with the specific antibody to Enc-1/NRP/B (dil 1:250, BD Biosciences, CA, USA) for 1 h at room temperature. Following incubation with secondary antibodies coupled to horseradish peroxidase (Vector Laboratories, CA, USA) for 45 min at room temperature, proteins were visualized with the ECL-Plus detection system (GE Healthcare, UK), as described by the manufacturer. Polyclonal antibody against α-tubulin, kindly provided by Dr. Frank Solomon (MIT, USA), was used (1:3000 dilution) as an internal control for protein loading. The images were obtained using either X-ray film or STORM 840 PhosphorImager (Molecular Dynamics/GE Healthcare, UK).

2.13. Immunofluorescence

Cultured cells were seeded onto glass coverslips in a 24-well plate at a density of 10^4 cells/well and grown for 24 h. Cells were fixed and permeabilized with methanol (−20 °C) for 10 min and washed with PBS, incubated in blocking solution (PBS + 2% BSA, 1 h) and then incubated with the primary antibody (Enc-1/NRP/B, BD Biosciences, CA, USA), diluted 1:100 in blocking solution. The primary antibodies were detected with fluorescent labeled secondary antibodies (Vector Laboratories, Burlingame, CA) and DAPI was used for nuclear staining. The immunostained coverslips were mounted using Vectarshield (Vector) and were examined under a fluorescence microscope Nikon (TE-300). Images selected were representative of the majority of the cells present on each experiment ($n = 3$ experiments performed). Control experiments to test primary antibodies specificity included incubation with preimmune mouse sera.

2.14. Immunohistochemistry

The paraffin-embedded tumor samples were sectioned at 4 μm. Sections were placed on precoated slides, dried overnight at 37 °C and stored at 4 °C. For immunostaining, sections were incubated with a monoclonal NRP/B antibody (dil 1:100, BD Biosciences) and a secondary antibody conjugated with peroxidase and detected with 3,3′-diaminobenzidine (Vector). For conventional histology, the neighboring sections were stained with hematoxylin and eosin (Vector).

2.15. Statistical analysis

Commercially available statistical software (PRISM v4.0, GraphPad Software Inc.) was used. The statistical analysis was submitted to one-way ANOVA, followed by the Tukey's test (non-parametric ANOVA). Differences were considered to be statistically significant at $P < 0.05$.

2.16. Accession numbers

Rat *Nrp/b* gene has been deposited in the GenBank with accession number AY669396 and protein rat NRP/B sequence with accession number AAT75221.

3. Results

3.1. Cloning and characterization of the full-length rat Nrp/b cDNA

The transcript product of the *Homo sapiens Nrp/b* sequence (gi 4505460) was subjected to a Blast search in the NCBI/GenBank™ database. Several rat ESTs mapping on rat chromosome 2 were identified with significant homology to the N- and C-termini of mouse and human *NRP/B* ORF. Based on the cDNA sequence inferred from searching the databases, we designed primers to isolate the coding region of the putative rat ortholog of *NRP/B*. cDNA was synthesized from total RNA isolated from C6/ST1 cells treated with Hy and used as template to amplify the putative 1,769 bp rat *Nrp/b* cDNA by PCR. This cDNA contains an ORF which encodes 589 amino acids with a predicted molecular mass of 66.126 Da and pI of 6.37. To amplify the rat full-length sequence corresponding to *Nrp/b* transcript, we used long-distance PCR and specific primers, which were designed based on rat ESTs (deposited at GenBank) from a cDNA library generated from C6/ST1 cells. The PCR product was sonicated and sequenced. The 4.5 kb cDNA sequence obtained, corresponding to the putative full length of rat *Nrp/b* gene, was deposited in the GenBank database under the accession number AY669396.

The genomic organization obtained for this rat *Nrp/b* transcript is summarized in Fig. 1 based on the alignment of the obtained cDNA sequence with rat genome. The rat *Nrp/b* gene spans an extension of approximately 12.3 kb of genomic sequence and its intron–exon boundaries closely resemble the human and mouse NRP/B gene (data not shown). Like the human and mouse *NRP/B* structure, the rat *Nrp/b* contains three exons.

Based on the protein sequence identity to human and mouse NRP/B (99%) (Fig. 2), and the similar protein architecture among the molecules, the newly identified protein was named rat Nrp/b. The rat Nrp/b (AAT75221) protein has the same two major structural elements found in the human and mouse sequences, namely the N-terminal BTB/POZ motif and the C-terminal kelch motif.

3.2. Distribution of Nrp/b expression in rat tissues and regulation of Nrp/b mRNA by GC treatment of C6/ST1 cells

The expression profile of the rat *Nrp/b* gene, examined by qRT-PCR in a panel of cDNAs obtained from eight different rat tissues, showed that *Nrp/b* is highly expressed in normal brain tissue (Fig. 4), presenting a lower expression in liver, followed by lung, testis, skeletal muscle, heart and kidney.

We previously reported on identification of a rat EST similar to the 3′ end of the *Nrp/b* gene, using Suppression Subtractive Hybridization (SSH) and mRNA prepared from the C6/ST1 cell line treated in the presence or in the absence of GC (100 ng/ml) [21]. This EST is detected as a single transcript of approximately 5.5 kb, which is induced upon a 5 h hydrocortisone (Hy) treatment [21]. Kinetic analysis of Hy-responsiveness by Northern blot (Fig. 3) using the rat Nrp/b cDNA as a probe showed the same level of transcript induction (7-fold) upon a 5 h treatment and accumulation of the transcript during prolonged treatment (up to 24 h) (Fig. 3).

3.3. Nrp/b overexpression does not affect growth in monolayer but inhibits anchorage independence

In order to assess the functional role of *Nrp/b* gene on the phenotypic reversion of rat glioma cell line, C6/ST1 cells were transduced with the pLPCX-NRP/B retroviral construct (described in Section 2) and then selected with Puromycin for 3 days. Northern blot analysis confirmed overexpression of the *Nrp/b* mRNA in exponentially growing C6/ST1 cells transduced with pLPCX-NRP/B, and no expression in parental cells or in C6/ST1 transduced with the empty vector or with the pLPCX-EGFP constructs (Fig. 5A). Western blot analysis confirmed Nrp/b overexpression at the protein level (Fig. 5B). In order to confirm the overexpression of rat *Nrp/b*, we assessed NRP/B expression by immunofluorescence in C6/ST1 cells transduced with the Nrp/b retrovirus. Fig. 5C shows the immunofluorescence pattern of C6/ST1 and C6/ST1-NRP/B cells labeled with specific monoclonal antibody to NRP/B-Enc-1. NRP/B was distributed throughout the cytoplasm in positive cells with the level of expression being higher in C6/ST1 cells transduced with retrovirus containing *Nrp/b* gene (C6/ST1-NRP/B) when compared to parental C6/ST1 cells, thus confirming N/RP overexpression in these cells.

To further explore the effect of NRP/B overexpression on C6/ST1 cells growth, the different populations of C6/ST1 cells transduced either with pLPCX-NRP/B, or the empty pLPCX vector or the pLPCX-EGFP construct were cultured for 9 days and the number of cells was periodically determined (Fig. 6). These results indicate that no major difference was observed in the growth curves either in the absence or in the presence of glucocorticoid (Hy). Under the microscope, no obvious difference was observed in cell morphology among these three groups. Flow cytometry and MTT assay were performed too and no differences were detected at growth rate

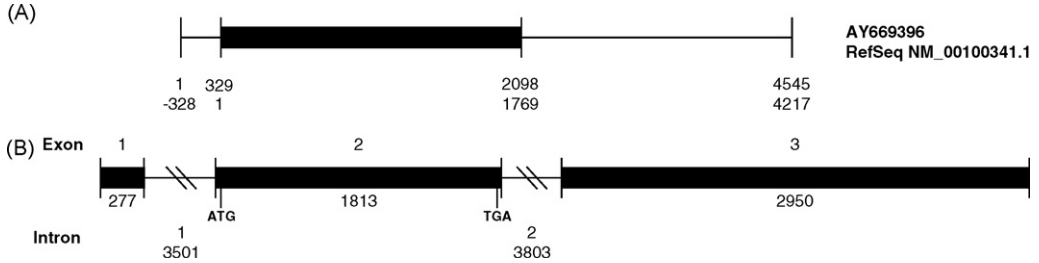

Fig. 1. Identification of rat *Nrp/b* gene. (A) The structure of rat *Nrp/b* cDNA. The open-reading frame of *Nrp/b* is indicated by a black rectangle. On the right, accession numbers for cDNA sequence are shown. (B) Diagram for rat *Nrp/b* gene structure. Boxes represent exons with the position of initiation and termination codons indicated. The scale shown applied only to exons; the entire region spans more than 12 kb of genomic DNA. The three exons and two introns are numbered and their size in base pairs is indicated below.

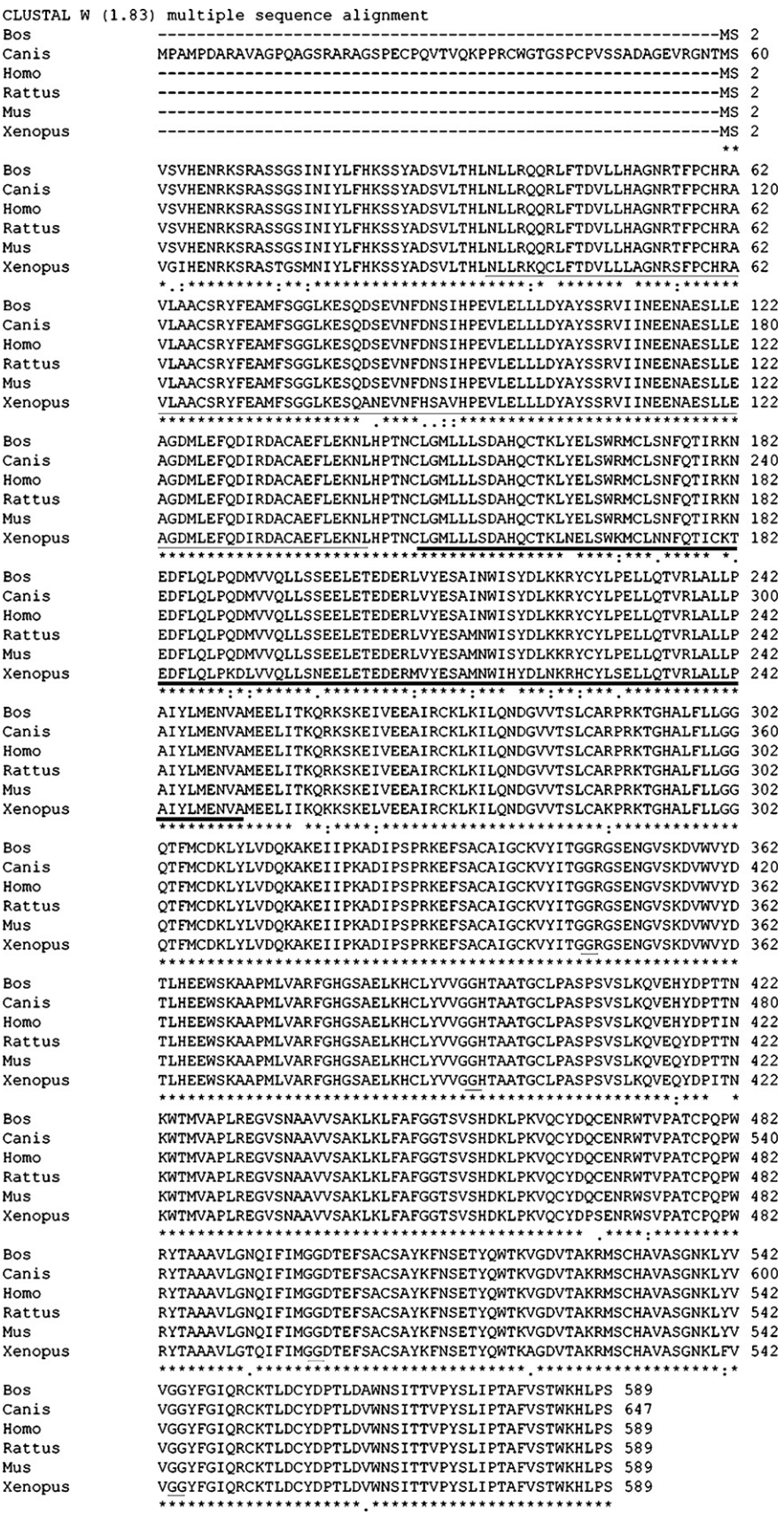

Fig. 2. Sequence alignment of rat NRP/B (gi50347091) protein with its orthologs. The alignment was generated using the Clustal W (1.85) program. The organisms and corresponding accession numbers used for this analysis are as follows: *Homo sapiens* (gi4505461); *Bos taurus* (gi76652957); *Canis familiaris* (gi73950299); *Mus musculus* (gi40254359) and *Xenopus laevis* (gi148229757). Numbers give the position of residues in proteins in relation to the first methionine of the NRP/B sequence. Amino acid residues with "*" are identical; conserved residues are represented by "**:**" and residues showing semi-conserved substitutions are represented by "**.**". The thin trace above the sequence denotes the BTB/POZ domain; the thick traces indicates the BACK domain and the small traces denote the double-glycine motif found in all Kelch repeats domain.

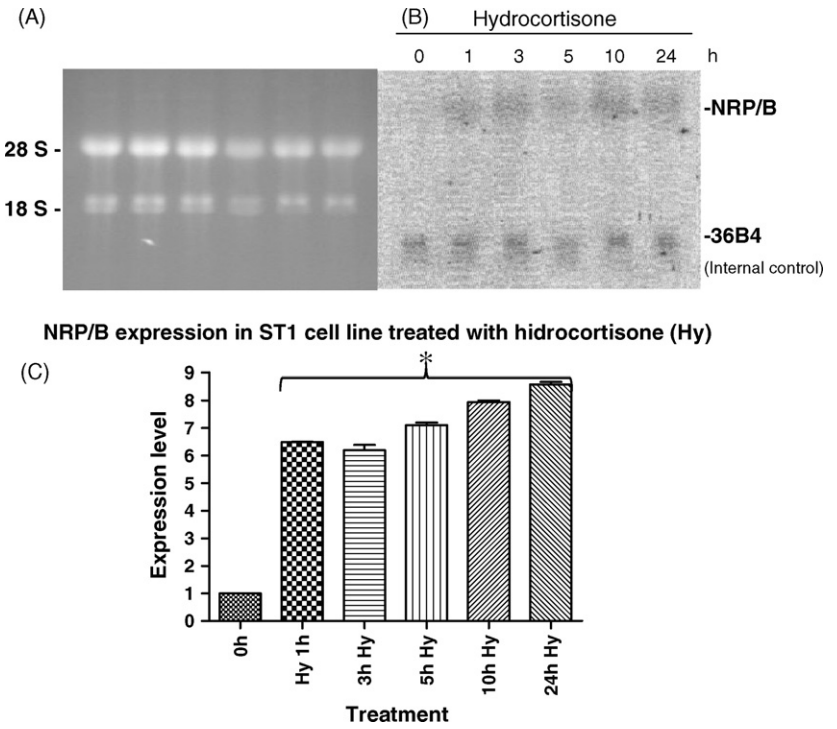

Fig. 3. Kinetic analysis of hydrocortisone-responsive *Nrp/b* expression by Northern blot. Cultures of C6/ST1 cells were serum-starved (0.2% FCS for 24 h) followed by treatment with hydrocortisone (100 ng/ml) for 1, 3, 5, 10 and 24 h. Samples of total RNA (20 μg) were purified, fractionated (A), blotted onto nylon membranes and hybridized to the radioactively labeled Nrp/b cDNA probe. 28 and 18S rRNA are indicated in formol-agarose gel (A). 36B4 expression was used as an internal standard (B). A and B are representative figures. All signals on the blot were quantified using a STORM 840 Phosphor Imager, and relative expressions are the values obtained relative to 36B4 expression levels and C6/ST1 without treatment (0 h) (C). $^{*}P < 0.001$ ($n = 3$).

(data not shown). These results indicated that upregulated NRP/B overexpression did not directly affect cell proliferation in monolayer cultures.

Anchorage-independent growth is considered to be the *in vitro* equivalent of tumorigenesis *in vivo*, therefore, NRP/B overexpressing C6/ST1 cells were also examined for anchorage-independent growth in a semi-soft agarose medium. C6/ST1 cells transduced with empty vector (pLPCX) or EGFP exhibited anchorage-independent growth in soft-agar similar to C6/ST1 parental cells (Fig. 7). However, C6/ST1-NRP/B cells displayed a significantly decreased ($P < 0.05$) in the ability to form colonies in agarose when compared with parental C6/ST1 cell line, suggesting a positive cor-

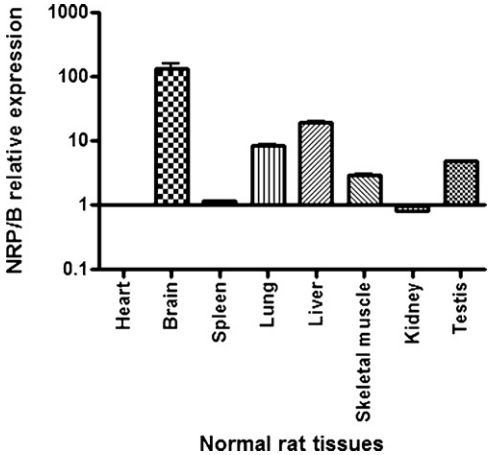

Fig. 4. mRNA expression levels of rat *Nrp/b* in cDNA samples from eight different rat tissues (heart, brain, spleen, lung, liver, skeletal muscle, kidney and testis) were analyzed by qRT-PCR. Relative expressions levels were normalized against the values obtained to *Gapdh* gene expression levels and heart gene expression values ($n = 3$).

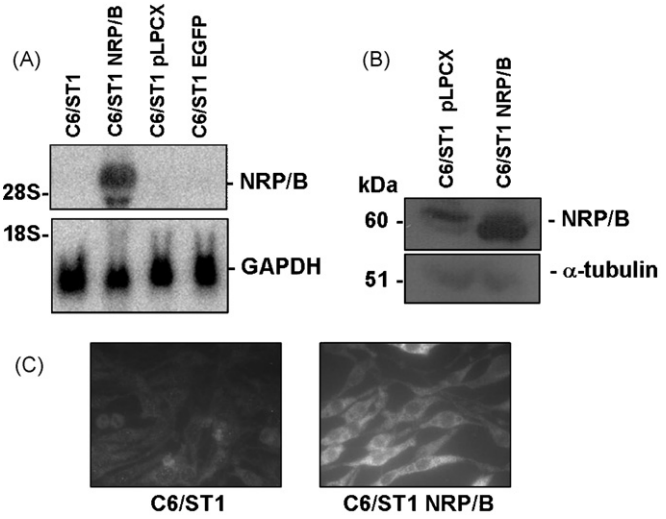

Fig. 5. Nrp/b overexpression in C6/ST1 cells. (A) Expression of Nrp/b in transduced C6/ST1 cells by Northern blot analysis: equal amounts of RNA were loaded, transferred to nylon membranes and hybridized with radioactively labeled Nrp/b and Gapdh cDNAs probes and analysed using a STORM 840 Phosphor Imager. Lane C6/ST1: total RNA from C6/ST1 parental cell line in exponential growing; lane C6/ST1-NRP/B: total RNA from pLPCX-NRP/B-transduced cells; lane C6/ST1-pLPCX: total RNA from pLPCX-transduced cells; lane C6/ST1-EGFP: total RNA from pLPCX-EGFP-transduced cells ($n = 3$). (B) Expression of NRP/B protein in transduced C6/ST1 cells by Western blot analysis: equal amounts of proteins were loaded and analyzed using NRP/B monoclonal antibody and α-tubulin polyclonal antibody as internal control. Lane C6/ST1-pLPCX: total cells lysates prepared from pLPCX-transduced C6/ST1 cells; lane C6/ST1-NRP/B: total cell lysates prepared from pLPCX-NRP/B transduced cells ($n = 3$). (C) Representative field of NRP/B expression demonstrated by immunofluorescence: upper panel shows C6/ST1 cells; lower panel shows cells transduced with pLPCX-NRP/B retrovirus ($n = 3$).

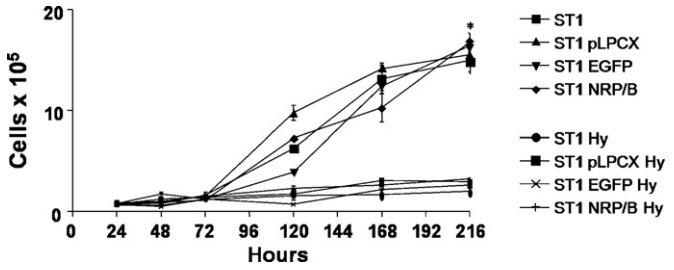

Fig. 6. Cell growth curves of C6/ST1 and C6/ST1 transduced cells with pLPCX, pLPCX-EGFP and pLPCX-NRP/B constructs treated or not with hydrocortisone (Hy). $P < 0.05$ at 216 h point of cell growth ($n = 3$).

relation between NRP/B expression and decreased survival/growth advantage of C6/ST1 cells under anchorage-independent conditions.

3.4. NRP/B overexpression leads to decreased tumorigenicity of C6/ST1 cells

Since NRP/B overexpression decreased the ability of C6/ST1 cells to grow in soft-agar, we investigated whether NRP/B overexpression would also alter the ability of these cells to form tumors in athymic nude mice. The same number (2.0×10^6) of C6/ST1-NRP/B, C6/ST1-EGFP, C6/ST1-pLPCX and C6/ST1 parental cells were injected subcutaneously into each of four Balb/c athymic mice in each group ($n = 2$). The animals were monitored for tumor growth during 6 weeks. The result obtained in two independent experiments shown in Fig. 8, indicated that both the frequency of tumor formation and the average tumor size were decreased at 6 weeks in mice injected with the C6/ST1-NRP/B cells, when compared with tumors induced by C6/ST1 parental cells, or by C6/ST1-EGFP or C6/ST1-pLPCX cells. Among the eight animals injected with the C6/ST1-NRP/B cells, just one mouse showed tumor growing with

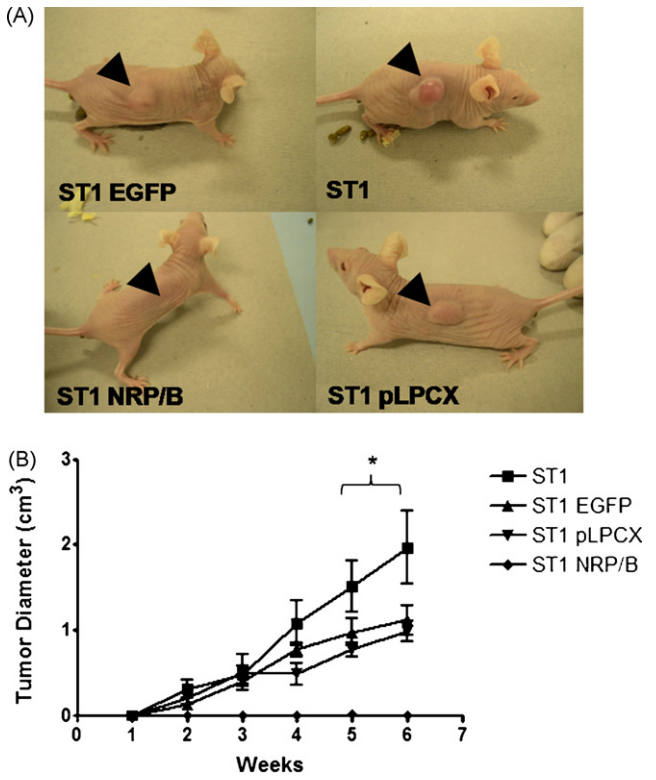

Fig. 8. Effect of the retroviral mediated transfer of *Nrp/b* gene on tumor growth *in vivo*. (A) Representative athymic mice showing tumor growth by C6/ST1 cells. Mice were individually injected subcutaneously with C6/ST1 cells (2×10^6 in 100 μl DMEM) and monitored for tumor growth for 6 weeks. Mouse injected with C6/ST1, C6/ST1-EGFP and C6/ST1-pLPCX show large tumor and mouse injected with C6/ST1-NRP/B show a small tumor. (B) Graph shows volume (cm^3) of tumors during 6 weeks from C6/ST1, C6/ST1-NRP/B, C6/ST1-EGFP and C6/ST1-pLPCX cells. *$P < 0.05$: comparing ST1-NRP/B volume tumor with others from 5th week.

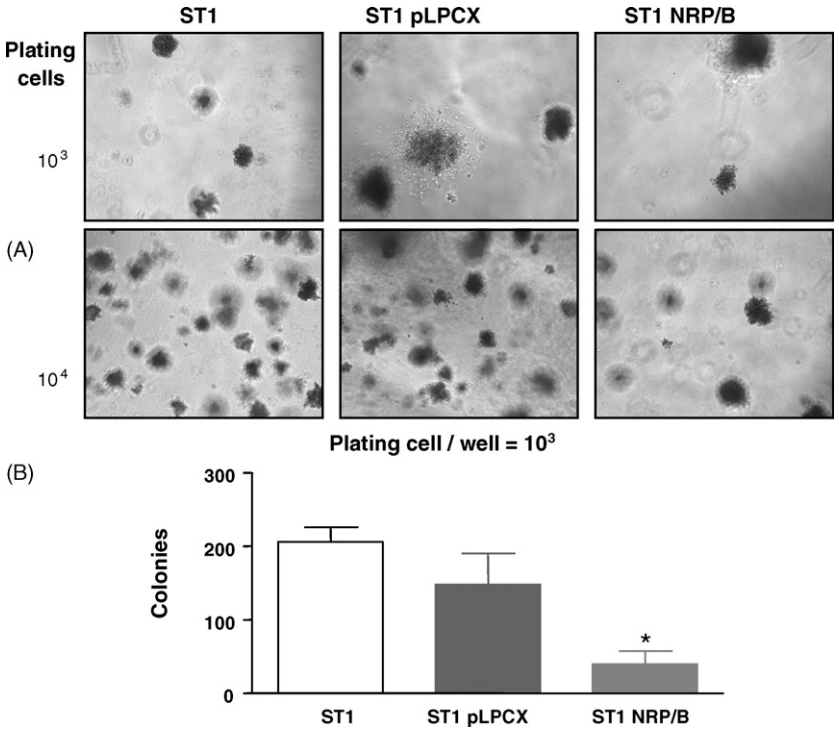

Fig. 7. Growth in agarose suspension of C6/ST1 cells and transduced cells with empty vector (pLPCX) and pLPCX-NRP/B construction. (A) 10^3 and 10^4 cells were plated per well (24 wells plate) following the protocol detailed in Section 2. (B) Effect of NRP/B overexpression in C6/ST1 cells on colony growth rate in agarose suspension. Cells colony were scored by diameter using a microscope at 10× magnification as describe in Section 2. $P < 0.05$ ($n = 3$).

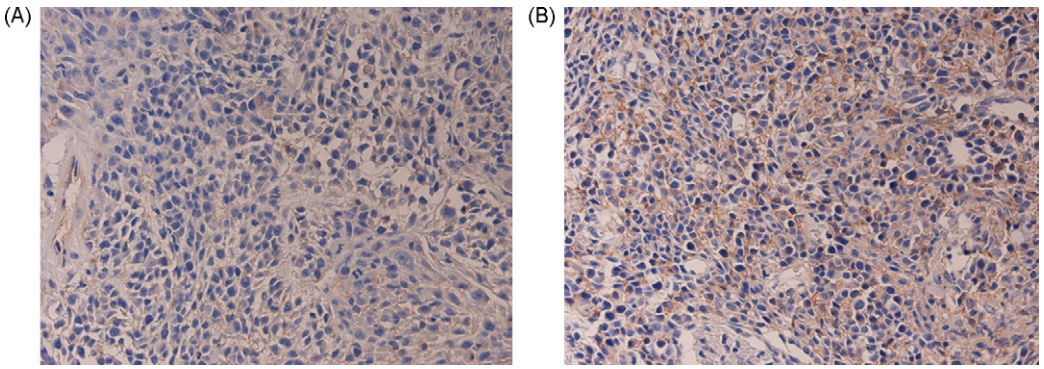

Fig. 9. Immunohistochemistry staining analysis of NRP/B protein in tumors originate from transduced C6/ST1 cells with empty vector (pLPCX) and pLPCX-NRP/B construction. (A) ST1-pLPCX cells. (B) ST1-NRP/B cells showing NRP/B positive-staining mainly localized in the cytoplasm. Original magnification: 400×.

small size. Control mice injected with DMEM only did not show any tumor growth during the observation period (data not shown). At the end of 6 weeks, the mice were sacrificed and the tumors were harvested and immediately included in paraffin blocks for immunohistochemistry.

3.5. Histological and immunohistochemical analysis of the only tumor formed from C6/ST1-NRP/B

To determine whether the lower tumorigenicity was, in fact, induced by overexpression of the rat *Nrp/b*, we examined the expression of NRP/B by immunohistochemistry in the single C6/ST1-NRP/B tumor formed in comparison with other tumors induced by C6/ST1-pLPCX cells. Histopathological analysis (by H&E staining) of samples taken from tumor tissues revealed no apparent differences in tissue architecture and morphology among all groups of mice studied, with tumor cells from all xenografts displaying similar structure. Localization of NRP/B was observed only in the cytoplasm of cells derived from C6/ST1-NRP/B tumor formed (Fig. 9).

4. Discussion

In the present study, we isolated and characterized the full-length cDNA sequence and elucidated the general genomic structure of the rat *Nrp/b* gene. We isolated and fully sequenced a cDNA clone with an insert size of 4,545 bp containing an open-reading frame of 1,769 bp in length and a 5′ noncoding region of 0.3 kbp and 3′ noncoding region of 2.4 kbp. Alignment of the product of rat *Nrp/b* with its orthologs, including *H. sapiens*, *Mus musculus*, *Bos taurus*, *Canis familiars* and *Xenopus laevis* indicates a strong aminoacid sequence conservation as well as similarity in size. In particular, the amino acid sequence identity between rat, human and mouse NRP/B is 99%. All of the differences are conservative amino acid changes, indicating that this gene is highly conserved among different species. Like its homologs, the N-terminal sequence of the rat Nrp/b displays a characteristic BTB/POZ domain and the C-terminal half of the protein contains six tandemly repeated kelch motifs. The BTB (Broad Complex, tramtrack and bric à brac) [53] or POZ (poxviruses and zinc finger) [54] is an evolutionarily conserved protein–protein interaction domain, which is found at the N-terminus of around 5–10% of the zinc finger transcription factors (reviewed in Collins et al. [55]) and in some actin-binding proteins having a kelch motif (reviewed in Albagli et al. [35]). Kelch repeats occur as 5–7 tandem copies, which form a β-propeller structure that interacts with actin filaments [25,56]. A BACK domain [57], is also found in the *Nrp/b* sequence playing an important structural and/or functional role in Cullin 3-mediated protein degradation.

In adult human tissues, NRP/B has been reported to be highly expressed in human brain and to display low expression in pancreas [23,58]. Our analysis of the expression of *Nrp/b* in rat tissues by qRT-PCR confirms that the corresponding *Nrp/b* mRNA is most abundantly expressed in brain tissue and at low levels in liver, lung, testis and skeletal muscle, but not in other tissues, such as spleen, heart and kidney (Fig. 4). Similar results were obtained by Zhao et al. [34] using Northern blotting, showing that *Enc-1* mRNA was highly expressed in brain and at lower levels in testis, adipocite tissues, but not expressed in adrenal, spleen, kidney, liver, muscle, heart, lung and intestine tissues. Abundant NRP/B signal expression was obtained in the cytoplasmic fraction and a weaker signal in the nuclear matrix and cytoskeleton-associated and nuclear proteins fractions of C6/ST1 cells [22]. The NRP/B protein was found to co-localize with actin in Daoy cells [25] and in preadipocytes [34] and in the nucleus, as part of the nuclear matrix [23,24]. In brain tumors, NRP/B diffused expression is described mainly in the cytoplasm [38,42], in agreement with the immunocytochemistry results we obtained with cells transduced with the NRP/B retrovirus (Fig. 5).

GCs have a potent anti-proliferative effect on astrocytes [59] and on some glioma cell lines [16]. GCs have been used for more than 40 years in the treatment of intracranial gliomas, however the exact molecular mechanisms by which glucocorticoids affect tumor growth, reduce tumor-associated edema and improve patient's clinical status are still largely unknown [60]. Dexamethasone treatment of rat hippocampus results in elevated levels of p53, suggesting p53 to be a player in GR-mediated growth arrest [61]. Recent results obtained in our laboratory demonstrate enhancement of p53 activity with inhibition of cell proliferation upon glucocorticoid receptor activation in C6/ST1 cells (data not shown). Kinetic analysis of C6/ST1 cells Hy-responsiveness showed elevate expression of the Nrp/*b* gene upon a 5 h of treatment with this GC hormone (Fig. 3), confirming the results previously obtained in our laboratory [21]. *Nrp/b* was first detected as a "p53-induced genes" or PIGs in colorectal cancer cell line transfected with p53 [26] and other p53 gene-targets were induced by Hy in ST1 cells, such as trombospondin-1 and cyclin G [21], suggesting growth arrest mediated by Hy via p53 activation.

In our study, the full-length rat *Nrp/b* cDNA was transduced into the C6/ST1 glioma cell line, and stable cell lines expressing the NRP/B protein were confirmed by immunofluorescence and Western blotting. Despite the high levels of this gene in these cells, no direct effect of *Nrp/b* was observed in cell proliferation in monolayer cultures (Fig. 6). However, C6/ST1-NRP/B cells displayed a significantly decreased ability to grow in soft-agar suspension, when compared with parental C6/ST1 cells or with cells overexpressing the EGFP protein or transduced with the empty vector pLPCX (Fig. 7), suggesting a diminished tumorigenic capacity of these cells, which was further supported by the tumor formation assays in

nude mice (Fig. 8). When subcutaneously injected into nude mice, the tumorigenicity of the only tumor formed from NRP/B overexpressing cells line was only 25–30% of that displayed by both the C6/ST1 parental cells and by cells transduced with the empty retroviral vector pLPCX or with the vector carrying only the EGFP gene (Fig. 8). Differently from normal cells, which require adherence to a substratum for growth [62,63], transformed cells usually grow in agarose suspension (anchorage independence), an ability which strongly correlates with tumorigenesis *in vivo* [64–66]. Anchorage dependence for growth is confined to the G1 phase of the cell cycle [67]. Once cells pass the restriction point, they no longer require adhesion to a substratum to complete the cycle [68]. Restoration of anchorage dependence to the C6/ST1-NRP/B cell line may be due to the effect of NRP/B on limiting the number of cells passing beyond the G1 phase, an effect which is similar to that of C6/ST1 cells upon treatment with hydrocortisone [46]. Kim et al. suggest that the growth suppressive effect of NRP/B may occur through interaction of its BTB-domain with $p110^{RB}$ or possibly through other key cell cycle regulatory proteins, such as E2F or the CDKs [36]. Previous results show that *in vivo* phosphorylation of NRP/B is regulated during cell cycle progression and that overexpression of NRP/B induces hypophosphorylation of $p110^{RB}$ during neuronal differentiation [23]. There is an induction of $p110^{RB}$ hypophosphorylation associated with NRP/B overexpression and, consequently, the cell cycle re-enter could not be promoted by E2F, an important transcription factor that regulate necessary genes for cell cycle progression, which is released when $p110^{RB}$ is phosphorylated. It is widely known that abnormalities in molecular regulators of the G1 checkpoint (p16/pRb/E2F pathway) are commonly present in most of human gliomas [2,69,70], therefore, it is important to develop more effective therapies which function by specifically targeting these signaling pathways (e.g., the excess of E2F1) malignant gliomas [71]. Taken together, our results imply that NRP/B plays a tumor suppressive role and may partly reverse the malignant growth potential of glioma cells both *in vitro* and *in vivo*.

In summary, we have cloned and characterized the glucocorticoid-regulated rat *Nrp/b* gene in the C6/ST1 glioma cell line. Our study underscores the functional importance of Nrp/b overexpression in limiting the tumorigenic potential of C6/ST1 cells, but further studies are required to characterize the signaling mechanisms underlying this effect and the exact role played by this gene during development of central nervous system.

Acknowledgements

We are deeply grateful to Zizi de Medonça, Patrícia Barros dos Santos, Sandra Regina de Souza, Débora Cristina da Costa, Ricardo Krett de Oliveira and Helena Medeiros for excellent technical assistance and to our lab colleagues for discussions and criticisms. We also thank Dra Leticia Labriola for critical review of the manuscript.

This work was supported by: FAPESP, CNPq, and PRP-USP.

References

[1] E.A. Maher, F.B. Furnari, R.M. Bachoo, D.H. Rowitch, D.N. Louis, W.K. Cavenee, R.A. DePinho, Malignant glioma: genetics and biology of a grave matter, Genes Dev. 15 (11) (2001) 1311–1333.
[2] K. Ichimura, H. Ohgaki, P. Kleihues, V.P. Collins, Molecular pathogenesis of astrocytic tumours, J. Neurooncol. 70 (2) (2004) 137–160.
[3] D.N. Louis, H. Ohgaki, O.D. Wiestler, W.K. Cavenee, P.C. Burger, A. Jouvet, B.W. Scheithauer, P. Kleihues, The 2007 WHO classification of tumours of the central nervous system, Acta Neuropathol. 114 (2) (2007) 97–109.
[4] E.P. Sulman, M. Guerrero, K. Aldape, Beyond grade: molecular pathology of malignant gliomas, Semin. Radiat. Oncol. 19 (3) (2009) 142–149.
[5] V.P. Collins, Gliomas, Cancer Surv. 32 (1998) 37–51.
[6] T.T. Huang, S.M. Sarkaria, T.F. Cloughesy, P.S. Mischel, Targeted therapy for malignant glioma patients: lessons learned and the road ahead, Neurotherapeutics 6 (3) (2009) 500–512.
[7] A.M. Sonabend, I.V. Ulasov, M.S. Lesniak, Gene therapy trials for the treatment of high-grade gliomas, Gene Ther. Mol. Biol. 11 (A) (2007) 79–92.
[8] T.J. Gill 3rd, G.J. Smith, R.W. Wissler, H.W. Kunz, The rat as an experimental animal, Science 245 (4915) (1989) 269–276.
[9] R.F. Barth, Rat brain tumor models in experimental neuro-oncology: the 9L, C6, T9, F98, RG2 (D74), RT-2 and CNS-1 gliomas, J. Neurooncol. 36 (1) (1998) 91–102.
[10] R.F. Barth, B. Kaur, Rat brain tumor models in experimental neuro-oncology: the C6, 9L, T9, RG2, F98, BT4C, RT-2 and CNS-1 gliomas, J. Neurooncol. (2009).
[11] B. Grobben, P.P. De Deyn, H. Slegers, Rat C6 glioma as experimental model system for the study of glioblastoma growth and invasion, Cell Tissue Res. 310 (3) (2002) 257–270.
[12] R.J. Grasso, Transient inhibition of cell proliferation in rat glioma monolayer cultures by cortisol, Cancer Res. 36 (7 (PT 1)) (1976) 2408–2414.
[13] J.E. Wolff, G. Molenkamp, M. Hotfilder, J. Laterra, Dexamethasone inhibits glioma-induced formation of capillary like structures in vitro and angiogenesis in vivo, Klin. Padiatr. 209 (4) (1997) 275–277.
[14] A.E. Nahaczewski, S.B. Fowler, S. Hariharan, Dexamethasone therapy in patients with brain tumors—a focus on tapering, J. Neurosci. Nurs. 36 (6) (2004) 340–343.
[15] D. Van Roost, A. Hartmann, G. Quade, Changes of cerebral blood flow following dexamethasone treatment in brain tumour patients. A Xe/CT study, Acta Neurochir. (Wien) 143 (1) (2001) 37–43 (discussion 43–34).
[16] B. Kaup, I. Schindler, H. Knupfer, A. Schlenzka, R. Preiss, M.M. Knupfer, Time-dependent inhibition of glioblastoma cell proliferation by dexamethasone, J. Neurooncol. 51 (2) (2001) 105–110.
[17] G.K. Whitfield, P.W. Jurutka, C.A. Haussler, M.R. Haussler, Steroid hormone receptors: evolution, ligands, and molecular basis of biologic function, J. Cell Biochem. Suppl. 32–33 (1999) 110–122.
[18] M.C. Armelin, H.A. Armelin, Glucocorticoid hormone modulation of both cell surface and cytoskeleton related to growth control of rat glioma cells, J. Cell Biol. 97 (2) (1983) 459–465.
[19] P. Benda, J. Lightbody, G. Sato, L. Levine, W. Sweet, Differentiated rat glial cell strain in tissue culture, Science 161 (839) (1968) 370–371.
[20] M.C. Armelin, M.L. Oliveira, J.M. Mercado, R.M. Sasahara, S.R. Valentini, L.H. Carvalho, Molecular genetic approach to cell proliferation control and neoplasia, Braz. J. Med. Biol. Res. 29 (7) (1996) 911–919.
[21] C.G. Vedoy, M.C. Sogayar, Isolation and characterization of genes associated with the anti-tumor activity of glucocorticoids, Brain Res. Mol. Brain Res. 106 (1–2) (2002) 57–69.
[22] M.A. Demasi, W.R. Montor, G.B. Ferreira, D.C. Pimenta, L. Labriola, M.C. Sogayar, Differential proteomic analysis of the anti-proliferative effect of glucocorticoid hormones in ST1 rat glioma cells, J. Steroid Biochem. Mol. Biol. 103 (2) (2007) 137–148.
[23] T.A. Kim, J. Lim, S. Ota, S. Raja, R. Rogers, B. Rivnay, H. Avraham, S. Avraham, NRP/B, a novel nuclear matrix protein, associates with p110(RB) and is involved in neuronal differentiation, J. Cell Biol. 141 (3) (1998) 553–566.
[24] T.A. Kim, S. Ota, S. Jiang, L.M. Pasztor, R.A. White, S. Avraham, Genomic organization, chromosomal localization and regulation of expression of the neuronal nuclear matrix protein NRP/B in human brain tumors, Gene 255 (1) (2000) 105–116.
[25] M.C. Hernandez, P.J. Andres-Barquin, S. Martinez, A. Bulfone, J.L. Rubenstein, M.A. Israel, ENC-1: a novel mammalian kelch-related gene specifically expressed in the nervous system encodes an actin-binding protein, J. Neurosci. 17 (9) (1997) 3038–3051.
[26] K. Polyak, Y. Xia, J.L. Zweier, K.W. Kinzler, B. Vogelstein, A model for p53-induced apoptosis, Nature 389 (6648) (1997) 300–305.
[27] R. Berezney, D.S. Coffey, Identification of a nuclear protein matrix, Biochem. Biophys. Res. Commun. 60 (4) (1974) 1410–1417.
[28] G.S. Stein, J.L. Stein, J.B. Lian, A.J. Van Wijnen, M. Montecino, A. Javed, S.K. Zaidi, D. Young, J.Y. Choi, S. Pockwinse, Nuclear microenvironments: an architectural platform for the convergence and integration of transcriptional regulatory signals, Eur. J. Histochem. 48 (1) (2004) 65–76.
[29] J. Nickerson, Experimental observations of a nuclear matrix, J. Cell Sci. 114 (Pt 3) (2001) 463–474.
[30] K.M. Tsutsui, K. Sano, K. Tsutsui, Dynamic view of the nuclear matrix, Acta Med. Okayama 59 (4) (2005) 113–120.
[31] J.R. Davie, S. Samuel, V. Spencer, L. Bajno, J. Sun, H.Y. Chen, L.T. Holth, Nuclear matrix: application to diagnosis of cancer and role in transcription and modulation of chromatin structure, Gene Ther. Mol. Biol. 1 (1998) 509–528.
[32] D. Zink, A.H. Fischer, J.A. Nickerson, Nuclear structure in cancer cells, Nat. Rev. Cancer 4 (9) (2004) 677–687.
[33] P. Loidl, A. Eberharter, Nuclear matrix and the cell cycle, Int. Rev. Cytol. 162B (1995) 377–403.
[34] L. Zhao, F. Gregoire, H.S. Sul, Transient induction of ENC-1, a Kelch-related actin-binding protein, is required for adipocyte differentiation, J. Biol. Chem. 275 (22) (2000) 16845–16850.
[35] O. Albagli, P. Dhordain, C. Deweindt, G. Lecocq, D. Leprince, The BTB/POZ domain: a new protein–protein interaction motif common to DNA- and actin-binding proteins, Cell Growth Differ. 6 (9) (1995) 1193–1198.
[36] T.A. Kim, S. Jiang, S. Seng, K. Cha, H.K. Avraham, S. Avraham, The BTB domain of the nuclear matrix protein NRP/B is required for neurite outgrowth, J. Cell Sci. 118 (Pt 23) (2005) 5537–5548.
[37] J.P. Varkey, P.J. Muhlrad, A.N. Minniti, B. Do, S. Ward, The *Caenorhabditis elegans* spe-26 gene is necessary to form spermatids and encodes a protein similar

to the actin-associated proteins kelch and scruin, Genes Dev. 9 (9) (1995) 1074–1086.
[38] X.Q. Liang, H.K. Avraham, S. Jiang, S. Avraham, Genetic alterations of the NRP/B gene are associated with human brain tumors, Oncogene 23 (35) (2004) 5890–5900.
[39] S. Seng, H.K. Avraham, S. Jiang, S. Yang, M. Sekine, N. Kimelman, H. Li, S. Avraham, The nuclear matrix protein, NRP/B, enhances Nrf2-mediated oxidative stress responses in breast cancer cells, Cancer Res. 67 (18) (2007) 8596–8604.
[40] X.J. Wang, D.D. Zhang, Ectodermal-neural cortex 1 down-regulates Nrf2 at the translational level, PLoS One 4 (5) (2009) e5492.
[41] S.G. Kim, S.J. Jang, J. Soh, K. Lee, J.K. Park, W.K. Chang, E.W. Park, S.Y. Chun, Expression of ectodermal neural cortex 1 and its association with actin during the ovulatory process in the rat, Endocrinology (2009).
[42] S. Seng, H.K. Avraham, G. Birrane, S. Jiang, H. Li, G. Katz, C.E. Bass, R. Zagozdzon, S. Avraham, NRP/B mutations impair Nrf2-dependent NQO1 induction in human primary brain tumors, Oncogene 28 (3) (2009) 378–389.
[43] S.F. Altschul, T.L. Madden, A.A. Schaffer, J. Zhang, Z. Zhang, W. Miller, D.J. Lipman, Gapped BLAST and PSI-BLAST: a new generation of protein database search programs, Nucleic Acids Res. 25 (17) (1997) 3389–3402.
[44] W.J. Kent, BLAT—the BLAST-like alignment tool, Genome Res. 12 (4) (2002) 656–664.
[45] R. Chenna, H. Sugawara, T. Koike, R. Lopez, T.J. Gibson, D.G. Higgins, J.D. Thompson, Multiple sequence alignment with the Clustal series of programs, Nucleic Acids Res. 31 (13) (2003) 3497–3500.
[46] M.C. Armelin, R.C. Stocco, H.A. Armelin, Control of rat C6 glioma cell proliferation: uncoupling of the inhibitory effects of hydrocortisone hormone in suspension and monolayer cultures, J. Cell Biol. 97 (2) (1983) 455–458.
[47] J.M. Chirgwin, A.E. Przybyla, R.J. MacDonald, W.J. Rutter, Isolation of biologically active ribonucleic acid from sources enriched in ribonuclease, Biochemistry 18 (24) (1979) 5294–5299.
[48] B. Ewing, P. Green, Base-calling of automated sequencer traces using phred. II. Error probabilities, Genome Res. 8 (3) (1998) 186–194.
[49] B. Ewing, L. Hillier, M.C. Wendl, P. Green, Base-calling of automated sequencer traces using phred. I. Accuracy assessment, Genome Res. 8 (3) (1998) 175–185.
[50] D. Gordon, C. Abajian, P. Green, Consed: a graphical tool for sequence finishing, Genome Res. 8 (3) (1998) 195–202.
[51] T.D. Schmittgen, Real-time Quantitative PCR Methods (San Diego, CA), vol. 25 (4), 2001, pp. 383–385.
[52] N. Jin, W. Chen, B.R. Blazar, S. Ramakrishnan, D.A. Vallera, Gene therapy of murine solid tumors with T cells transduced with a retroviral vascular endothelial growth factor—immunotoxin target gene, Hum. Gene Ther. 13 (4) (2002) 497–508.
[53] G. Pengue, V. Calabro, P.C. Bartoli, A. Pagliuca, L. Lania, Repression of transcriptional activity at a distance by the evolutionarily conserved KRAB domain present in a subfamily of zinc finger proteins, Nucleic Acids Res. 22 (15) (1994) 2908–2914.
[54] S. Zollman, D. Godt, G.G. Prive, J.L. Couderc, F.A. Laski, The BTB domain, found primarily in zinc finger proteins, defines an evolutionarily conserved family that includes several developmentally regulated genes in Drosophila, Proc. Natl. Acad. Sci. U.S.A. 91 (22) (1994) 10717–10721.
[55] T. Collins, J.R. Stone, A.J. Williams, All in the family: the BTB/POZ, KRAB, and SCAN domains, Mol. Cell Biol. 21 (11) (2001) 3609–3615.
[56] J. Adams, R. Kelso, L. Cooley, The kelch repeat superfamily of proteins: propellers of cell function, Trends Cell Biol. 10 (1) (2000) 17–24.
[57] P.J. Stogios, G.G. Prive, The BACK domain in BTB-kelch proteins, Trends Biochem. Sci. 29 (12) (2004) 634–637.
[58] M.C. Hernandez, P.J. Andres-Barquin, I. Holt, M.A. Israel, Cloning of human ENC-1 and evaluation of its expression and regulation in nervous system tumors, Exp. Cell Res. 242 (2) (1998) 470–477.
[59] K.L. Crossin, M.H. Tai, L.A. Krushel, V.P. Mauro, G.M. Edelman, Glucocorticoid receptor pathways are involved in the inhibition of astrocyte proliferation, Proc. Natl. Acad. Sci. U.S.A. 94 (6) (1997) 2687–2692.
[60] C. Piette, C. Munaut, J.M. Foidart, M. Deprez, Treating gliomas with glucocorticoids: from bedside to bench, Acta Neuropathol. 112 (6) (2006) 651–664.
[61] O.F. Almeida, G.L. Conde, C. Crochemore, B.A. Demeneix, D. Fischer, A.H. Hassan, M. Meyer, F. Holsboer, T.M. Michaelidis, Subtle shifts in the ratio between pro- and antiapoptotic molecules after activation of corticosteroid receptors decide neuronal fate, FASEB J. 14 (5) (2000) 779–790.
[62] J.E. Meredith Jr., B. Fazeli, M.A. Schwartz, The extracellular matrix as a cell survival factor, Mol. Biol. Cell 4 (9) (1993) 953–961.
[63] D.G. Stupack, X.S. Puente, S. Boutsaboualoy, C.M. Storgard, D.A. Cheresh, Apoptosis of adherent cells by recruitment of caspase-8 to unligated integrins, J. Cell Biol. 155 (3) (2001) 459–470.
[64] M.A. Cifone, In vitro growth characteristics associated with benign and metastatic variants of tumor cells, Cancer Metastasis Rev. 1 (4) (1982) 335–347.
[65] V.H. Freedman, S.I. Shin, Cellular tumorigenicity in nude mice: correlation with cell growth in semi-solid medium, Cell 3 (4) (1974) 355–359.
[66] I. Macpherson, L. Montagnier, Agar suspension culture for the selective assay of cells transformed by Polyoma virus, Virology 23 (1964) 291–294.
[67] R.K. Assoian, Anchorage-dependent cell cycle progression, J. Cell Biol. 136 (1) (1997) 1–4.
[68] R.M. Bohmer, E. Scharf, R.K. Assoian, Cytoskeletal integrity is required throughout the mitogen stimulation phase of the cell cycle and mediates the anchorage-dependent expression of cyclin D1, Mol. Biol. Cell 7 (1) (1996) 101–111.
[69] D.N. Louis, Molecular pathology of malignant gliomas, Annu. Rev. Pathol. 1 (2006) 97–117.
[70] D.N. Louis, J.F. Gusella, A tiger behind many doors: multiple genetic pathways to malignant glioma, Trends Genet. 11 (10) (1995) 412–415.
[71] M.M. Alonso, R. Alemany, J. Fueyo, C. Gomez-Manzano, E2F1 in gliomas: a paradigm of oncogene addiction, Cancer Lett. 263 (2) (2008) 157–163.